Bottom design optimisation of electric arc furnace for ferromanganese production using nodal wear model

R. Parra[1], J. Mochón[2], R. Martín D.*[2], J. I. Verdeja[3], M[a]. F. Barbés[3], L. F. Verdeja[3], N. Kanari[4] and I. Ruiz-Bustinza[2]

This paper presents the optimisation on the design of the lining of an electric arc furnace that produces refined ferromanganese by applying the nodal wear model. This model is a new tool that systematises the wear/corrosion analysis applied to industrial furnaces linking the basic theoretical knowledge of the physical chemistry of wear/corrosion phenomena and the industrial conditions. The use of this tool to optimise the process helped increase the number of tappings between furnace bottom rebuilds from 19 in 1999 to 1200 in 2005 and the productivity to increase from 1·2 to 2·7 ton h^{-1}.

Keywords: Electric arc furnace, Ferromanganese, Corrosion, Mathematical modelling NWM

Introduction

The world steel production is currently around 1350 Mt/year. Manganese is a classic alloying element but the demand for low nitrogen, hydrogen and boron in certain grades has increased the demand for refined and electrolytic manganese in recent years.

The wear of the electric arc furnace (EAF) bottom, where this refining process is carried out, has been analysed from the beginning of the operation in order to extend the number of tappings and to increase productivity. This analysis, design and optimisation was made applying the nodal wear model (NWM) which is a new tool that combines the physical chemistry of wear/corrosion phenomena with the lining geometric description using finite element grid mathematical modelling. A first presentation of the model and some applications were published in 2005.[1] The present work extends the one case study presentation to explain in details the application of the NWM.

Wear/corrosion phenomena in lining of pyrometallurgical reactors

The wear/corrosion of a ceramic material depends on many different parameters that have been widely studied at laboratory scale. Those studies give a reasonable understanding and quantification of the physical chemistry phenomena and allow expression, in most of the cases, of a rate of dissolution of the material that is tested. This phenomenological and/or semi-empirical approach was developed by Cooper and Kingery,[2–4] Hrma[5] and Cook.[6] Nevertheless, these results cannot be applied directly to other configurations than those used for their derivations and the experimental conditions where they were applied. The mathematical description also gives equations to evaluate the dynamic evolution of a liquid that infiltrates in a porous media for the infiltration phenomena.

The lining of a pyrometallurgical reactor is a complex structure where the direct application of those equations does not represent the real wear and corrosion phenomena that take place in it. We can say that every material has a specific behaviour depending on the liquid with which it contacts and the temperature at the interface.

The NWM proposes a methodology for a systematic analysis of the wear/corrosion processes that take place in the lining of a furnace from a comprehension of the fundamental mechanism determined at laboratory scale and applying it as close as possible the real conditions during operations. The concept of this analysis is to combine three levels of knowledge: the experimental and laboratory tests, the theoretical and phenomenological description of the wear/corrosion, and the mathematical modelling. This sequence is a classical methodology for process modelling, but not yet applied to wear and corrosion simulation. The two first points allow proposition of the control step for the physical chemical wear/corrosion phenomena. The mathematical modelling gives a tool to simulate different designs for the lining and different operational conditions.

To achieve the analysis a precise determination of the temperature at the interface liquid/lining is needed. As

[1]Departamento de Ingeniería Metalúrgica (DIMET), Casilla 160-C. Correo 3. Concepción. Universidad de Concepción, Chile
[2]Centro Nacional de Investigaciones Metalúrgicas (CSIC/CENIM), Avda. de Gregorio del Amo, 8. 28040 Madrid, Spain
[3]Departamento de Ciencia de los Materiales e Ingeniería Metalúrgica, Grupo de Investigación en Siderurgia, Metalurgia y Materiales (SID-MET-MAT). Escuela de Minas. Independencia s/n. 33004 Oviedo, Universidad de Oviedo, Spain
[4]Laboratoire Environnement et Minéralurgie, UMR 7569 CNRS, Nancy-University, ENSG, BP 40, 54501 Vandoeuvre-lès-Nancy Cedex, France

*Correspondence author, email rmduarte@wanadoo.es

Published by Maney on behalf of the Institute
Received 18 December 2008; accepted 28 February 2009
DOI 10.1179/174328109X443329

explained later, this temperature is obtained by a finite element method (FEM) solution of the thermal field where the nodes of the FEM grid represent the lining geometry and a temperature in each node of the liquid/lining interface calculation. The obtained temperature is called the nodal temperature Ti, and so on. Each property for the lining or the fluid (gas, slag and metals) at each node in the interface is calculated.

The NWM has been successfully applied for corrosion test simulation at laboratory scale and for the design of furnace linings at industrial scale.[7–9] From these applications the NWM proposes two basic and specific new approaches for the classical analysis of the wear/corrosion phenomena in industrial furnaces:

(i) the laboratory test extrapolations for the materials selection that will be used in a furnace lining are traditionally based on the material identification with the higher resistance to attack by the melt. In some cases, this criterion allows a good selection, but it is accepted that the solution most of the time has shortcomings requiring further trial and error tests. Applying the NWM, a material selection is based on its dynamic behaviour calculated from the simulation. Some wear/corrosion could be observed, for example, at the beginning of the operation, but eventually a degree of equilibrium is attained. Certainly the conditions to reach this equilibrium depend on the total relining design of the furnace and not only on the selection of the material with which contacts the melt

(ii) the 'working temperature' at the interface has been traditionally considered as the process temperature, that could be measured directly T_∞. This differs from the Nodal temperature T_i, which is not possible to be measured directly. The difference between both temperatures $(T_\infty - T_i)$ could increase many tens of degrees even if the thermal boundary layer is small.[10,11]

$$T_i = T(x_i, y_i, z_i)$$

$$T_\infty = T(x_i + \delta_x, y_i + \delta_y, z_i + \delta_z)$$

(The calculations are explained further in the text, $\delta_x = \delta_y = \delta_z$).

All the parameters and variables that influence wear and corrosion are a function of T_i and $(T_\infty - T_i)$. To apply the NWM a thermal field must be calculated in the lining. The mathematical solution for this problem was developed by means of a finite element model with two boundary conditions: the temperature at the shell or the temperature of the bath T_∞, and the heat transfer between the melt and the lining, represented by the convective heat transfer coefficient. With these two known parameters and the thermal conductivity λ for the materials used in the lining, the complete thermal field can be calculated including the nodal temperature T_i.[9]

Formalism of model[1]

During refining operations the wear/corrosion phenomena modifies the geometry of the lining. The thermal field before a Δt, which could represent a cycle of operation, is no longer valid since a new geometry appears and the temperature distribution is left consolidating along this new geometry of the refractory lining. The geometry modification is calculated for each node in the interface melt/refractory by a corrosion equation based on L/t . This equation, characterised by the control mechanism of the wear process is an empirical equation based on the phenomenological analysis of the wear phenomena that allows defining the control mechanism of this very complex process. The parameters of this corrosion/wear equation are calculated from the T_i, $(T_\infty - T_i)$ and $T_i - T_{i-1}$ and $T_i - T_{i+1}$ values that are the thermal difference between the node i and their adjacent ones. With this formulation, the corrosion rate in the node i expressed in units of length by unit of time is represented by equation (1)

$$v(corrosion)_i = f(T_i; T_i - T_\infty; T_i - T_{i-1}; T_i - T_{i+1}); \left[\frac{L}{t}\right] \quad (1)$$

The wear in each node is determined supposing that the temperature remains constant during the interval of time Δt

$$(Wear)_i = v(corrosion)_i \Delta t; \ [L] \quad (2)$$

As the geometry of the system has been modified, the new temperature field should be obtained solving the same FEM problem with a new geometry. The evolution of the wear/corrosion profile for the lining is obtained by means of an iterative process. If each iterative cycle takes place after a certain Δt, the calculation process for the i node in the nth iteration is:

(i) temperature in the i node by FEM: $T_{i,n-1}$

(ii) corrosion rate in the node i: $v(corrosion)_i = f(T_{i,n-1}; \Delta T_{i.n-1})$

(iii) wear during the Δt of the iteration n in the i node: $(Wear)_i = v(corrosion)_i \Delta t$

(iv) definition of the new geometry and calculation of the new temperature field $T_{i,n}$ in the whole refractory lining, and hence the nodal temperature (temperature at the melt/refractory interface).

It is important to note that the melt/refractory interface, where the attack occurs, defines a surface build by the nodes where the wear/corrosion equations are applied. This two-dimensional grid is independent of the FEM grid used for the numeric resolution of the temperature field in the lining.

To apply the NWM it is necessary to develop corrosion equations $[v(corrosion)_i]$ that allow the geometry correction of the refractory lining. These equations depend on the specific mechanism considered as control step of the lining corrosion/wear. For the furnace simulation and design presented, two basic mechanisms were considered: infiltration in the open porosity for the furnace original refractory (castable or sintered) and chemical dissolution for the modified furnace bottom.

Infiltration

The simplification in the representation of the porous refractory microstructure as a straight line pore of radius r is very useful for the derivation of the thermodynamic and kinetic expressions for pore infiltration. The equilibrium value of liquid rise in this capillary can be calculated by minimising the variation in total free energy ΔF as a function of the rise z. Setting $d(\Delta F)/dz = 0$, the following equation is obtained, giving the equilibrium rise z_e

$$z_e \rho g - \frac{2\sigma_{lv}\cos\theta}{r} = P_o - P_v \quad (3)$$

where ρ is the liquid density, g the gravity, σ_{lv} the surface energy between the liquid and the gas phase, θ the wetting angle between the liquid and the solid, P_o the pressure applied on the liquid at the capillary entrance $z=0$ and P_v the pressure of the vapour phase ahead of the infiltration front.

If it is assumed that the flow of the infiltrated melt is incompressible and laminar with viscosity η, the velocity u can be expressed by

$$u = \frac{dz}{dt} = -\frac{1r^2 dP}{\eta 8\, dz} = \frac{1r^2 \Delta P_t}{\eta 8 \quad z} \quad (4)$$

The total pressure drop driving infiltration is equal to the applied pressure $P_o - P_v$ minus the capillary pressure $\Delta P_c = \frac{2\sigma_{lv}\cos\theta}{r}$, and minus the hydrostatic pressure $\rho g z$. In most practical situations, $z \ll z_e$, so ΔP_t is nearly constant during the infiltration process ($\Delta P_t \approx P_o - P_v - \Delta P_c$). After integrating equation (4) once with respect to z and then with respect to time taking $z=0$ at $t=0$, it gives

$$z = \left[\frac{r^2}{4\eta}\right]^{1/2} \Delta P_t^{1/2} t^{1/2} \quad (5)$$

Applying equation (5), also known as Washburn's equation, to an industrial furnace where the height of the liquid metal and slag represents the metallostatic pressure, it can be transformed in a unidirectional equation (L/t) to apply in each of the nodes of the surface for the melt/lining interface.

$$v(corrosion)_i = \frac{2(\rho_S g z_S + \rho_M g z_M + P_{atm})^2}{\gamma_{m/g}\cos\theta\eta} r^2;\ \left[\frac{L}{t}\right] \quad (6)$$

Assuming that the melt in the furnace are metal and a slag, the parameters of equation (6) are: ρ_S the slag density, z_S slag eight, ρ_M metal density, z_m metal eight and P_{atm} the atmospheric pressure over the bath.[9–12]

Chemical dissolution

The chemical dissolution takes place when one of the refractory constituents can be dissolved in the melt. To obtain the nodal equation, the dissolution is considered as a process where a refractory constituent diffuses into the melt. If any chemical reaction occurs at the interface it is not taken into account due to the high rate of chemical reactions at high temperature, and so no chemical control is expected. The basic equations that represent these phenomena are Fick's laws of mass transfer. For a steady state condition the diffusional mass flow of the attacked species J_i, could be calculated by the well known equation

$$J_i = k_i \Delta C_i \quad (7)$$

where k_i is the mass transfer coefficient, ΔC_i the concentrations difference of the species that diffuses between the interface and the melt bulk.

This equation can be transformed to represent this control mechanism, in units of length by unit of time

$$v(corrosion)_i = k_i \Delta C_i \left(\frac{\rho_i}{\rho_g}\right)\left(\frac{100}{\%cm}\right);\ \left[\frac{L}{t}\right] \quad (8)$$

In equation (7) the difference of concentration ΔC_i should be expressed as a fraction; ρ_i is the nodal density of the melt in contact with the refractory; ρ_g is the bulk density of the refractory and $\%cm$ is the percentage of the constituent that dissolves. The value for the nodal mass transfer coefficient from the refractory surface to the melt is obtained by the following equation

$$k_i = 0{\cdot}332 Re^{1/2} Sc^{1/3} \left(\frac{D_i}{L}\right) \quad (9)$$

where D_i is the diffusion coefficient or the attacked species, L the lineal characteristic dimension, Re the Reynolds number and Sc the Schmidt number, both of which are chosen as the most representative of the conditions in the interface refractory/melts in the furnace.

The corrosion equation that results from substituting the equation (9) in (8) is

$$v(corrosion)_i = 0.332 Re^{1/2} Sc^{1/3} \left(\frac{D_i}{L}\right)\left(\frac{\rho_i}{\rho_g}\right)\left(\frac{100}{\%cm}\right);\ \left[\frac{L}{t}\right] \quad (10)$$

To be able to use this corrosion equation it is necessary to know the movement of the melt at the interface with the refractory. The nodal velocity $\bar{v}_i$ used to calculate the Reynolds number is estimated from specific conditions where the equation will be applied. Table 1 summarises the equations used in this study.[9]

Analysis and optimisation of EAF lining

The furnace has an internal diameter of 4·24 m. and a sole with a diameter of 2·40 m (Figs. 1 and 2). The initial furnace bottom was made with a castable refractory with high MgO content (>95%), as shown in Fig. 2. The average duration for this first design was only 19 tappings, which represent a corrosion rate of 0·52 cm h^{-1}. When the sole thickness reached the security refractory level (sintered magnesite, Fig. 2) the furnace was cooled for the reinstatement with a new sole. The corrosion rate is extremely high if it is compared with the corrosion rate of a furnace sole producing carbon steel ($3{\cdot}70 \times 10^{-2}$ cm h^{-1}). This initial

Table 1 Corrosion equation applied in nodal wear model

Mechanism	Equation
Infiltration	$v(corrosion)_i = \frac{2(\rho_S g z_S + \rho_M g z_M + P_{atm})^2}{\gamma_{m/g}\cos\theta\eta} r^2;\ \left[\frac{L}{t}\right]$
Chemical dissolution	$v(corrosion)_i = 0.332 Re^{1/2} Sc^{1/3}\left(\frac{D_i}{L}\right)\left(\frac{\rho_i}{\rho_g}\right)\left(\frac{100}{\%cm}\right);\ \left[\frac{L}{t}\right]$

1 Electric arc furnace for refined ferromanganese production

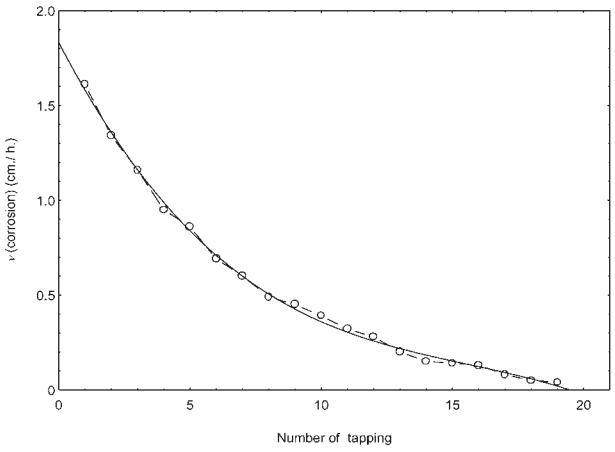

3 Measured corrosion rate for magnesite monolithic refractory (MgO>95%) in central node, point 1 (0,0), Fig. 2

condition in 1999 pushed the authors to analyse the possible optimisation using the NWM.

Calculation of convective heat transfer coefficient between melt and refractory

For the original lining the infiltration by the FeMn was identified as the control step for the wear/corrosion phenomenon. The first calculation was carried out in order to adjust the unknown parameters to the evolution of the wear, as shown in Figs. 3 and 4. The calculation used the $v(corrosion)$ of equation (6) to fit the curve for the central node (point 1 (0,0), Fig. 2). The parameters used were the following:

(i) surface tension of the ferroalloy:[13,14] from the values for the pure metals, Fe and Mn, and with the supposition of the same behaviour that for the Cr–Fe system, where the surface tension of Fe diminishes with chromium addition, it is assumed that for the manganese the surface tension diminishes due to the presence of 20%Fe and the value of 1·0 N m^{-1} is retained

(ii) slag density:[14] 3200 kg m^{-3}, constant for the calculation

(iii) ferromanganese density (kg m^{-3}):[13,14] ρ(Fe–80Mn)=7125–0·893T (K)

(iv) contact angle of the ferromanganese in the refractory:[13,14] $\sigma=30^{\circ}$

(v) average of thermal conductivity of refractory materials in the bottom:[14] (λ=10 W m^{-1} K^{-1})

(vi) average size of porous in the central zone: 10 μm

(vii) total height of the melt in the central node: 0·34 m

(viii) the viscosity was expressed as a function of temperature. The solidification interval was measured using differential thermal analysis. The liquidus temperature is 1180°C and the solidification ends at 975°C, where a value for a rigid solid was considered. The value at 1100°C

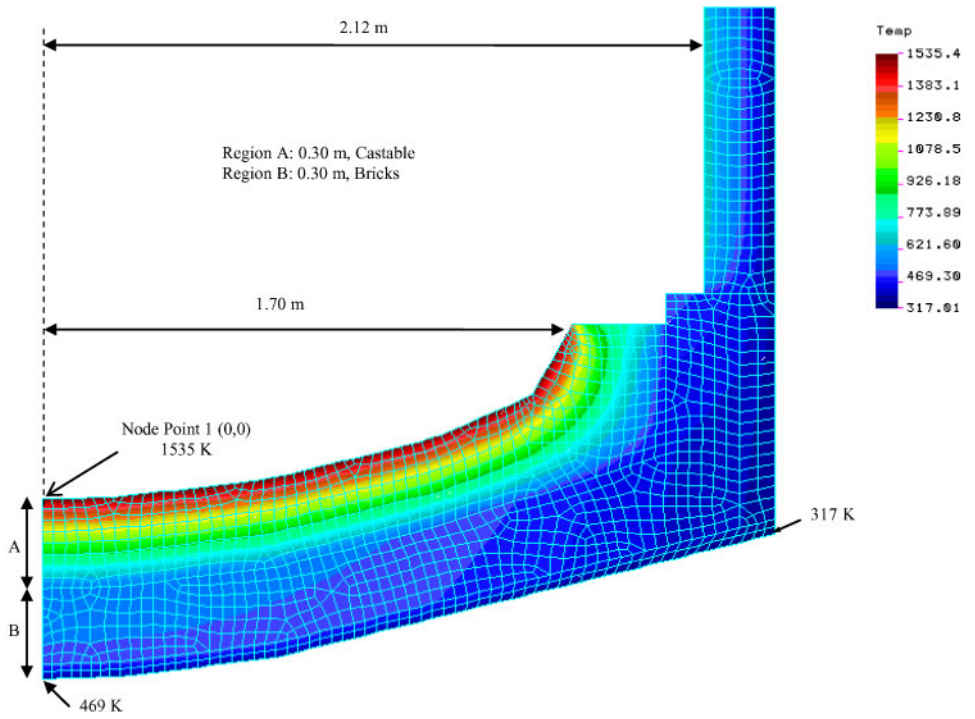

2 Geometry two-dimensional and thermal field for original lining design: temperature in shell is 460–317 K

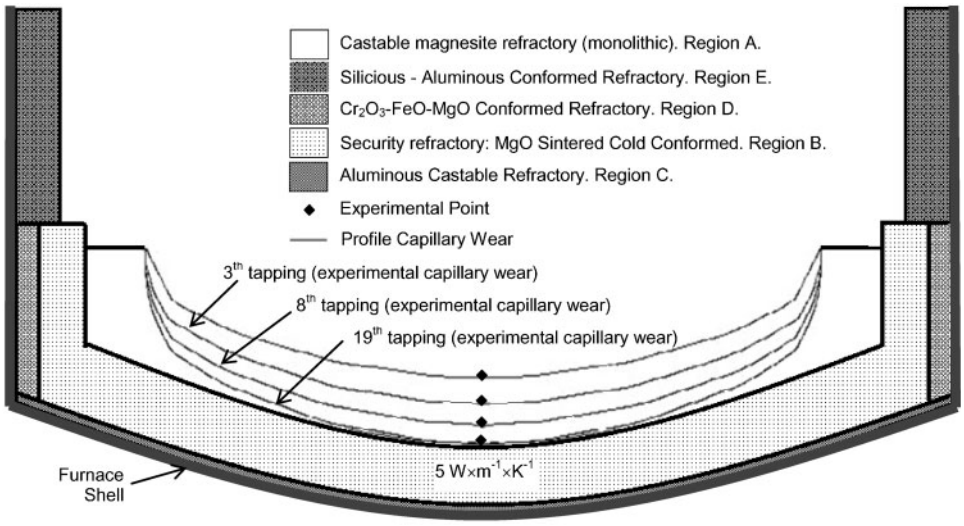

4 Measured and calculated wear/corrosion profile (capillary equation): lining is first used in EAF (1999) and adjustment of equation fits well with experimental results

was considered for a viscous flow or solid creep.[9,15] 1400°C was estimated from those of a manganese melt and the Fe–C system (there are not reported in the literature a specific value for the ferroalloy used in this study). Table 2 summarises the values used for the calculation.[9]

As outlined, the thermal field must be calculated using the appropriate boundary conditions. One of these conditions is the temperature or heat flux in the shell. The second is the heat transfer condition between the sole and the melt, which is determinate knowing the convective heat transfer coefficient between the liquid ferroalloy and the sole. As criteria to adjust the values of the penetration the thermal profile must reflect the penetration stop when the liquid solidifies at 1100°C. The problem is solved using FEM to find the evolution in the lining for the 1100°C isotherm. The value of 18 W m^{-2} K^{-1} adjusts the curve of Figs. 3 and 4, after 19 tappings, the residual thickness of the MgO sole with a tolerance of 5 mm reaches the security refractory (sintered magnesite, Figs. 2 and 4, region B). The value obtained for the convective heat transfer constitutes a fundamental reference for all the simulations. Since the physical chemistry properties of the ferroalloy, the operative conditions and the furnace dimensions remain the same this value is used for all the calculations. The values for the viscosity for 1119 and 1280°C (Table 2) were obtained as a corollary to confirm the wear profile as shown in Fig. 4.[9,15]

First optimisation of lining: changes in materials and design

The first idea to improve the initial very poor results was to change the heat transfer conditions by modifying the lining design. To achieve this objective, materials with a higher thermal conductivity were considered in the simulation. The bottom remains the same (Fig. 4, region A) and changes were introduced in the thermal conductivity for the materials in Fig. 4 (regions B–E).

Case 1

Region B (Fig. 4) changes from sintered magnesite (λ=11·0 W m^{-1} K^{-1}), to magnesia carbon graphite refractory (λ=25 W m^{-1} K^{-1}), as shown in Fig. 5.

Case 2

Regions B–D (Fig. 4) using a magnesia carbon graphite refractory (λ=25 W m^{-1} K^{-1}), as shown in Fig. 6.

The results for the corrosion profile with condition 1 are shown in Fig. 5 and for condition 2 in Fig. 6. In both cases, an improvement in the number of tapping was outlined. Case 1 achieved 25 tappings, case 2, 33 tappings.

Second optimisation of lining: change of furnace bottom

The second improvement in the lining design was the sole modification (region A, Figs. 2 and 4) in order to change the physical chemistry control of the wear/corrosion. When the sole is made of a castable dolomitic material with small average size particles (<100 μm) and low content of impurities (75%MgO, 20%CaO, 0·60%SiO_2, 3·80%Fe_2O_3, 0·30%Al_2O_3, others 0·30%), the formation of liquid reactive phases is facilitated at low temperature. The open porosity is very low and the corrosion mechanism is conditioned to the dissolution of the matrix constituent (magnesium, calcium, aluminium and iron silicates) in the melt. In this case, the constituent of the refractory that is corroded by the melt is the SiO_2 by the reactions

$$(SiO_2)_{matrix} + 2(Mn)_{Fe-Mn} = (\underline{Si})_{Fe-Mn} + 2(MnO_2)_{slag} \quad (11)$$

$$(SiO_2)_{matrix} + 2(\underline{C})_{Fe-Mn} = (\underline{Si})_{Fe-Mn} + 2(CO)_{gas} \quad (12)$$

It was shown experimentally that this substitution of the castable magnesite by a dolomitic sole increases the number of tapping to ~45. In this case, the corrosion rate is 0·27 cm h^{-1} (the 30 cm sole wear is achieved in 45 operations of 2·5 h each) and this value continues to

Table 2 Temperature, viscosity data for FeMn alloy: 80Mn–1·4C–0·8Si–0·15P–17·65Fe

Temperature, °C	975 (Ref. 15)	1100 (Ref. 15)	1119	1280	1400 (Ref. 12)
Viscosity, Pa s	$1·0 \times 10^{12·5}$	$1·0 \times 10^{8}$	$4·3 \times 10^{7}$	$8·2 \times 10^{5}$	$5·0 \times 10^{-3}$

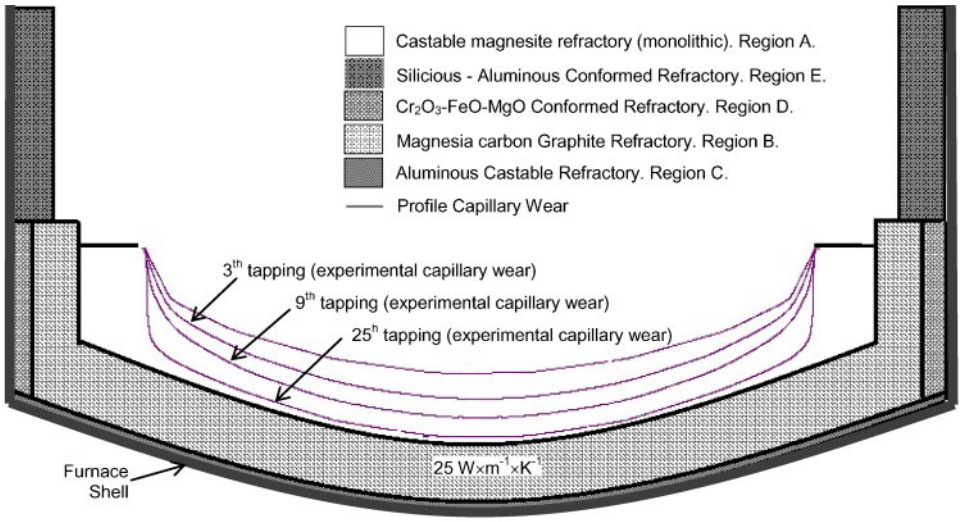

5 Wear profiles for magnesite refractories, case 1

be far from the value $3{\cdot}70\times10^{-2}$ cm h^{-1}, the case of an EAF sole in carbon steel production. In this case, the simulation procedure uses $v(corrosion)$ given by equation (10). To be able to use this corrosion equation it is necessary to know the melt movement in the interface with the refractory. The nodal velocity $\bar{v}_i$, used to calculate the Reynolds number is estimate from the two following considerations:

(i) the flotation equation of particles of density ρ_y and size D_p is

$$\bar{v}_i = g\frac{D_p^2}{18\mu}(\rho_m - \rho_p) \tag{13}$$

(ii) the thickness for the velocity boundary layer δ_v of a fluid that moves over a flat surface is

$$\delta_v = 5{\cdot}0\left(\frac{\mu L}{\bar{v}_i\rho}\right)^{1/2} \tag{14}$$

For the system under analysis, the followings can be identified:

a. the characteristic lineal dimension L, from equation (14) with δ_v ($L=\delta_v$)
b. the diameter of particles of Stokes equation, from equation (13) with δ_v ($D_p=\delta_v$)
c. the difference ($\rho_m-\rho_p$) from equation (13) with $\Delta\rho_{ii}$, difference between densities from i node and his adjacent.

Then, the velocity of the melt in the i node $\bar{v}_i$ (in m s^{-1})

$$\bar{v}_i = 6{\cdot}98\mu_i^{1/3}\rho_i^{-2/3}\Delta\rho_i^{1/3} \tag{15}$$

Substituting equation (15) in (10) the corrosion rate is obtained for every node in the melt/refractory interface, expressed (in m s^{-1})

$$v(corrosion)_i = 8.80\ 10^{-3}L^{-1/2}\left(\frac{\Delta\rho_i}{\rho_i}\right)^{1/6} D_i\Delta(\%\,C)_i\left(\frac{\rho_i}{\rho_g}\right)\left(\frac{100}{\%cm}\right) \tag{16}$$

where the concentration difference of the species that diffuses is expressed in percentage. For the dissolution of SiO_2 from the matrix of the new sole the equation (16)

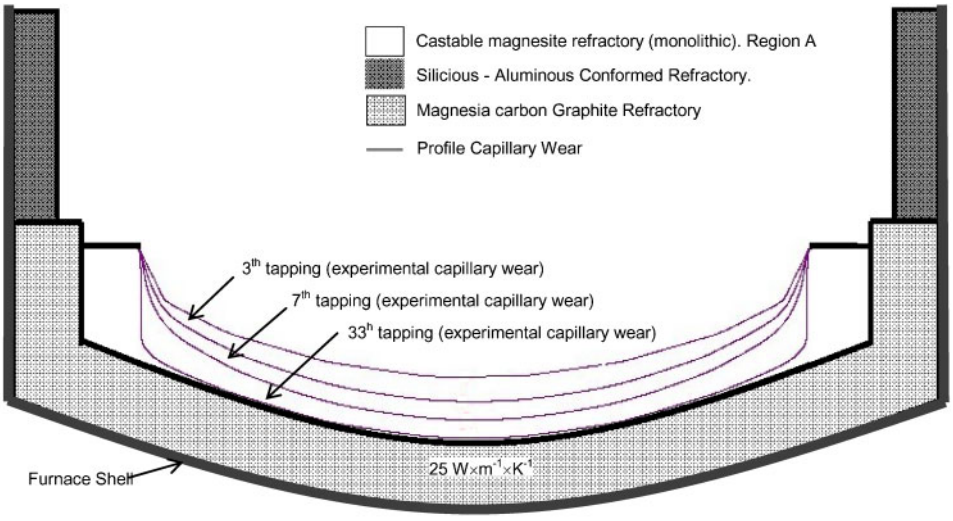

6 Wear profiles for magnesite refractories, case 2

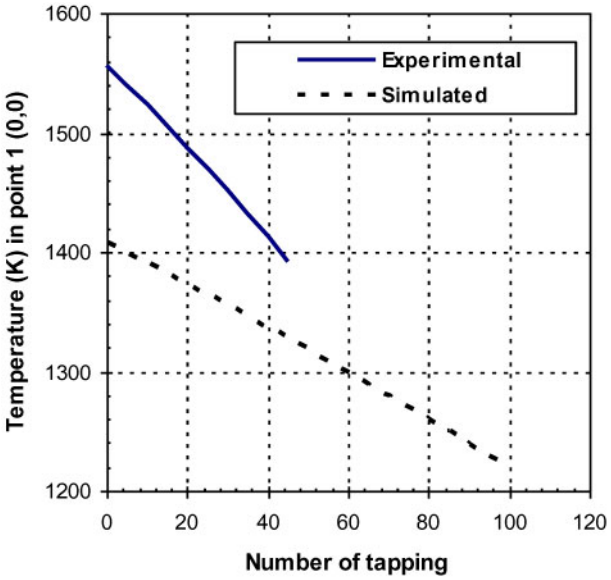

7 Experimental and simulated evolution for nodal temperature at point 1 (Figs. 2 and 3): simulation corresponds to heat loses increase from furnace

$$v(corrosion)_i = 7.65 \times 10^{-5} \left(\frac{9.0}{\rho_i}\right)^{1/6} D_{Si}^{2/3} (Si^{=} - Si^{0}) \rho_i \quad (17)$$

where:

(i) $9{\cdot}0$ kg m^{-3} is the difference of average densities between the central node and their adjacent ones during the 45 tappings

(ii) $7{\cdot}65 \times 10^{-5}$ is a constant that includes the value of $8{\cdot}80 \times 10^{-3}$ from equation (16), the value of the global density of the refractory, 2100 kg m^{-3}, the linear characteristic dimension for the furnace L, $1{\cdot}20$ m, and the 5% of the matrix constituent in the sole matrix

(iii) $D_{Si} = 4{\cdot}50 \times 10^{-7} \exp\left(-\frac{4626}{T(K)}\right)$ (m^2 s^{-1}). This values correspond to the approximation from the Fe–Si (0,0–4·0%) system to the ferromanganese alloy[13]

(iv) density of the ferromanganese (kg m^{-3}):[13,14] $\rho_i = 7125 - 0{\cdot}8393T$ (K)

(v) $S_i^0 = 0{\cdot}80\%$, silicon content in the melt in mass-%

(vi) S_i^m maximum silicon content in the melt in mass-% which corresponds to the thermodynamic equilibrium compositions from reactions (11) and (12).

In the same way to the previous infiltration control, the thermal problem resolution using FEM (with the boundary condition for the convective heat transfer coefficient 18 W m^{-2} K^{-1}) establishes a relation among the central node temperature (point 1 (0,0), Fig. 2) and the number of tappings. This representation was chosen because the problem has an additional degree of freedom such that the heat transfer coefficient remains the same as obtained from the previous analysis (infiltration control). This relation represents the effect of the geometry change by the successive sole corrosion profiles in the temperature.

In equation (17) all the parameters are known except S_i^{∞}. Assuming the chemical wear model one can adjust a relationship among S_i^{∞} and temperature that adjust the rate of wear in the central node. We obtained equation (18), the relationship that represents effectively the chemical equilibrium of reactions (11) and (12).

$$S_i^{=} = 32000 \exp\left(-\frac{2644}{T(K)} - 8{\cdot}20\right) \quad (18)$$

With the corrosion equation adjusted from the experimental data one can simulate different situations to improve the behaviour of the material used in the sole. If the central node temperature (point 1 (0,0), Fig. 2) follows the variation given by the simulated curve in Fig. 7, the corrosion average rate is $0{\cdot}12$ cm h^{-1} that represents 100 tappings. To obtain this profile the following actions were carried out:

(i) increasing the thermal conductivity of the materials that comprise the security lining: regions B–D in Fig. 4

(ii) increasing the external refrigeration conditions (air and water): forced convection of air or watering

(iii) using both mechanisms simultaneously.

Final situation: intensive shell refrigeration to increase heat loses

The actual lining design has take into account all the simulations done and the continuous modification that has optimised the number of tapping from 19 to >100. The new design considers air forced convection to increase the furnace refrigeration.[16] The results of this new design 2002 are shown in Table 3.

Conclusions

The evolution of the design and the operational results for the EAF are summarised in Table 3.

The optimisation was achieved by different actions that can be classified in three groups.

1. Diminishing of the nodal temperature, T_i at the refractory/liquid alloy interface. The actions were the use of materials with high thermal conductivity, an appropriate lining design to ensure a good heat transfer

Table 3 Summary of improvements in operation of EAF

Year	Tappings between sole reconstruction	Productivity, ton h^{-1}	Comments
1999	19	1·2	Capillary control of the wear corrosion phenomena. Magnesite sole
2000	45	1·44	Chemical control and castable dolomitic sole and higher conductivity in the security refractory.
2002	1200	2·7	Chemical control and castable dolomitic sole with intensive refrigeration on the shell.

from furnace to the surroundings and use of forced convection for the shell refrigeration.

2. Increasing the furnace power and the charging and tapping system.

3. Hot repair of the lining by 'ceramic welding' without any humidity bonding, accounting for 30% of the improvement.

Item 1 is directly related with the NWM, while items 2 and 3 are operational optimisations but related to the lining optimisation, as especially the power increase that needs a more reliable sole.

Outlook

Although the data represent an impressive optimisation, opportunities exist for further improvement. The simulation using the NWM has shown that the formation of a protective layer in the sole could further increase the number of tappings. One of the options is the use of carbide layers. The problem is to find in what conditions the nodal temperature T_i could be the equilibrium temperature for the following reaction

$$(Me_xC_y)_{solid} = x(\underline{Me})_{Fe-Mn} + y(\underline{C})_{Fe-Mn} \quad (19)$$

An evident problem is the chemical compatibility between the refined ferromanganeseand a solid protection layer on the sole.

Another way to improve the useful life could be a new design with materials that have higher thermal conductivity so as to further increase the heat loses and modify the thermal field. In the actual design, the temperature in the shell is $\sim 150^{\circ}C$, higher than $100^{\circ}C$ from the initial design. The aim would be to reach a nodal temperature near the solidus temperature of the ferroalloy, $\sim 900^{\circ}C$.

Acknowledgements

The authors thank Ferroatlantica Group (F. Fernández; J. C. Sánchez and J. Bullón) for the possibility to publish this work. Thanks to Education and Science Ministry of Spain (grant no. MAT2003-00502); Foreign Affairs and Cooperation Ministry of Spain (grant nos. MAEC-AECI-B/1629/04; B/2884/05; B/5814/06 and B/7648/07) and CENIM-CSIC-Madrid.

References

1. R. Parra, L. F. Verdeja, M♀ F. Barbés, Ch. Goñi and V. Bazán: 'Analyzing furnace-lining integrity using nodal wear modelling', *JOM*, 2005, **57**, (10), 29–36.
2. R. Cooper and W. D. Kingery: 'Dissolution in ceramic systems I : molecular diffusion, natural convection and forced convection studies of sapphire dissolution in calcium aluminum silicate', *J. Am. Ceram. Soc.*, 1964, **47**, (1), 37–43.
3. B. N. Samaddar, W. D. Kingery and A. R. Cooper: 'Dissolution in ceramic systems II: dissolution of alumina, mullite, anorthite and silica in a calcium–aluminium–silicate slag', *J. Am. Ceram. Soc.*, 1964, **47**, (5), 249–254.
4. Y. Oishi, A. R. Cooper and W. D. Kingery: 'Dissolution in ceramic systems III: boundary layer concentration gradients', *J. Am. Ceram. Soc.*, 1965, **48**, (2), 88–95.
5. P. Hrma: 'Contribution to the study of the function between the rate of isothermal corrosion and glass composition', *Verres Refract.*, 1970, **24**, (4–5), 166–168.
6. L. P. Cook, D. W. Bonnell and D. Rathnamma: 'Model for molten salt corrosion of ceramics', *Ceram. Trans*., 1990, **10**, 75–251.
7. L. F. Verdeja, R. Parra, M♀. F. Barbés, Ch. Goñi and V. Bazán: 'Application of the nodal wear model to the static finger test of refractories corrosion'. *Steel Grips*, 2005, **3**, (2), 105–110.
8. Ch. Goñi, M[a]. F. Barbés, V. Bazán, E. Brandaleze, R. Parra and L. F. Verdeja: 'The mechanism of thermal sapling in the wear of the Pierce-Smith copper converter', *J. Ceram. Soc. Jpn*, 2006, **114**, (8), 672–675.
9. L. F. Verdeja, J. P. Sancho and A. Ballester: 'Materiales Refractarios y Cerámicos', 156–176, 193–201; 2008, Síntesis, Madrid, España.
10. L. F. Verdeja, M[a]. F. Barbés, R. González, G. A. Castillo and R. Colás: 'Thermal modelling of a torpedo – car', *Rev. Metall. Madrid*, 2005, **41**, (6), 449–455.
11. N. Eustathopoulos, R. Parra and M. Sánchez: 'Role of capillarity in corrosion of refractories by melts', Proc. Int. Conf. Copper 2003, Santiago, Chile, November 2003, Vol. 4, No. (2), pp. 457–471.
12. E. W. Washburn: 'Dynamics of capillary flow', *Phys. Rev.*, 1921, **17**, 374–517.
13. Y. Kaway and Y. Shiraishi: 'Handbook of physico-chemical properties at high temperatures', 1988, 145–151, 173–178, 188; 1988, Tokyo, Iron and Steel Institute of Japan.
14. D. Springorum: 'Slag atlas', 313–349; 1995, Düsseldorf, Verein Deutscher Eisenhüttenleute (VDEh).
15. L. H. van Vlack: 'Elements of materials science and engineering', 6th edn, 349; 1990, New York, Addison-Wesley.
16. M[a]. F. Barbés, E. Marinas, E. Brandaleze, R. Parra, L. F. Verdeja, G. A. Castillo and R. Colás: 'Design of blast furnace crucibles by means of the nodal wear model', *ISIJ Int*., 2008, **48**, (2), 134–140.